

Syntheses, Characterizations, and Structures of a New Series of Aliphatic–Aromatic Polyesters. 1. The Poly(tetramethylene terephthalate dicarboxylates)

Mohamed Atfani and François Brisse*

Département de Chimie, Université de Montréal, C. P. 6128, Succ. Centre-ville, Montréal, Québec, H3C 3J7 Canada

Received August 12, 1999; Revised Manuscript Received August 14, 1999

ABSTRACT: A new family of polyesters, the poly(tetramethylene terephthalate dicarboxylates) of formula $[-O-CO-C_6H_4-CO-O-(CH_2)_x-O-CO-(CH_2)_y-CO-O-(CH_2)_x]_n$, was synthesized and characterized by 1H and ^{13}C NMR in $CDCl_3$ solution, infrared spectroscopy, molecular weight distribution, and X-ray fiber diffraction analysis. The 1H and ^{13}C NMR spectroscopy and the molecular weight distribution confirm the homogeneous alternating distribution of the two kinds of diacids (aromatic and aliphatic). The crystal structures of the adipate and the succinate were determined by interpretation of their X-ray diffraction patterns. A dynamic infrared spectroscopic study confirmed the existence of a nongauche–nontrans torsion angle in the glycol segments, while the diacid moieties were in a nearly all-trans conformation.

Introduction

In recent years there has been an increasing interest in developing biodegradable chemosynthetic polymers. The aliphatic polyesters constitute an important class of biodegradable polymers, but their thermal and mechanical properties are generally too poor for their use as such a material. Thus, the introduction of a terephthaloyl segment into the polyester backbone might lead to better physical properties as well as controlled degradability. It was reported that biodegradability of aliphatic/aromatic copolyesters is strongly affected by composition, sequence distribution, crystallinity, structures of crystallites, and melting temperatures.¹ Very few studies on biodegradation of the chemosynthetic aliphatic polyesters and their copolymers have been reported.^{2,3}

As polyesters readily transesterify, near and above their melting points, interchange reactions commonly occur between constituents.⁴ Results show that ester interchange is rapid in the melt, and ester interchange also takes place but is a lot slower 15 °C below the melting temperatures.⁵ Transreaction in polyester blends depends strongly on their initial compatibility and on the blending conditions. These include temperature, duration of mixing, preparation method, viscosity match, and the presence of catalysts and inhibitor. However, details of the process are not yet completely understood, and there is no complete agreement in the literature about the relative importance of the three possible mechanisms (alcoholysis, acidolysis, or direct ester exchange).⁶ Whatever the mechanism, it is generally agreed that the interchange reactions lead to the formation of a first block and then the random copolymers, which enhances the miscibility of the blend.

The degradation processes, syntheses, and properties of segmented block copolymers based on dimerized fatty acids with different molecular weights as the soft phase together with poly(tetramethylene terephthalate) as the hard phase were investigated.^{7,8} The multiblock structure of segmented block copolymers results from the crystallization ability of the hard segments dispersed in the amorphous matrix of soft segments. An interest-

ing dependence of the changes of the thermal properties on the mutual segment content, particularly on the crystalline phase in polyesters, and the degree of polycondensation of hard segment is observed.⁸ On transesterification, the physical properties and the constituents of the system change because of the production of new components. Several techniques have been used to detect these changes.^{7–9}

One of the most commonly used techniques is infrared spectroscopy, which originates from a molecular vibration that causes changes in the dipole moment and polarizability of the molecular chains.

1H and ^{13}C NMR spectroscopy are the most powerful tools available to analyze the sequence of polymer microstructure and to provide insight about the chemical changes within polyester pairs. The NMR spectroscopy was successfully used to analyze a wide variety of polyesters.⁹

In recent studies,¹⁰ the melt copolycondensation of poly(ethylene terephthalate), 2GT, with poly(ethylene succinate), PES, and that of poly(tetramethylene terephthalate), 4GT, with poly(tetramethylene succinate), PTMS or PES, were investigated by using a broad binary composition range of the considered polyesters. In these copolyesters, prepared by melt copolymerization at up to 270–300 °C and under reduced pressure, the authors observed a random distribution of the aliphatic and aromatic basic units. The composition of the different triad sequences was determined by 1H NMR in $CDCl_3$. Using X-ray diffraction, the authors noted that for a composition rich in the aromatic polyesters, the aromatic/aliphatic diad can cocrystallize by the incorporation of the aliphatic chain into the aromatic crystallites. On the other hand, for a composition rich in aliphatic polyesters, the insertion of the aromatic chains in the crystallites of the aliphatic polyesters is difficult because of the degree of randomness and block nature of polymers.

The random copolyesters prepared by transesterification of PTMS and 4GT, at 290 °C and under a reduced pressure, exhibited distinct melting endotherms related to the major component in the respective polyester.¹¹

This was also observed by X-ray diffraction: the peak positions in the X-ray diffractogram correspond to those of the homopolymer of the major component. These characteristic peaks of homopolymer disappeared after a longer reaction time.

It was reported¹² that the uniaxial stretching of poly(tetramethylene terephthalate) fibers is accompanied by a crystal-crystal transition. In the relaxed, or α -form of 4GT, the length of the molecular chain, or fiber repeat, is nearly 10% shorter than the value observed in the stretched or β -form. The $\alpha \rightarrow \beta$ transition of 4GT, produced by mechanical deformation (uniaxial stretching), is reversible, and only the α -form is stable in the relaxed state at room temperature.

Numerous X-ray structural studies have been reported^{13–18} for both crystal forms of 4GT. All the crystal structures proposed for the relaxed α -form approximate a gauche-trans-gauche conformation for the glycol residue, although there are small differences among them. In the case of the β -form, infrared and Raman spectroscopies^{19–23} suggest a nearly all-trans sequence for the glycol residue. X-ray studies were also undertaken; however, the published results show significant discrepancies.^{15–17} It is believed that the driving force behind the reversible transformation is the enhanced packing efficiency of the terephthalate groups in the α -phase.

X-ray studies of aliphatic polyesters with smaller repeating units have revealed a shortening of the c -axis dimension as compared to that based on an all-trans planar zigzag conformation.^{24–28} Gauche as well as trans conformations were found in the crystalline domains of 2–4, 2–6 and 2–8 polyesters.^{23,26} The c -axis dimension of PTMS, is 10.79 Å, that is, 1.41 Å shorter than the value calculated for an all-trans conformation (12.20 Å).²⁹ A new crystal modification, strain induced, was found in uniaxially oriented fibers of PTMS,³⁰ and the crystal transition mechanism between the α and β forms was investigated.³¹ The molecular conformation of the α form is t_7gtg^- , where t , g , and g^- denote trans, gauche, and gauche⁻ torsion angles, respectively. On the other hand, the molecular conformation of the β form is zigzag planar (t_{10}). For poly(tetramethylene adipate), PTMA, two distinct crystalline forms (monoclinic and orthorhombic) were also reported.³² The chain conformation in both forms is zigzag planar, nearly but not quite all-trans.

To combine the properties of the aromatic and aliphatic polyesters, a new series of aromatic-aliphatic polyesters with flexible spacers and regular alternation was synthesized and its properties were investigated, $[-O-CO-C_6H_4-CO-O-(CH_2)_x-O-CO-(CH_2)_y-CO-O-(CH_2)_z]_n$. These polyesters include two kinds of acid segments, an aromatic terephthalate and a linear dicarboxylate. These aromatic-aliphatic polyesters should combine some of the properties of the two polyesters from which they are derived. Melting points, rigidity of the chain, solubility, etc. are expected to have intermediate values.

We have undertaken to examine the series of poly(tetramethylene terephthalate dicarboxylates). The polyesters were synthesized in a two-step procedure starting with dimethyl terephthalate, the relevant aliphatic diol ($x = 2, 4, 6$), and the aliphatic diacid ($y = 2, 4, 6, 8$). All the polyesters thus synthesized were characterized by ¹H and ¹³C NMR in solution in CDCl₃ and by infrared spectroscopy, melting point and density determinations, and molecular weight distribution.

In the present work, we specifically report on the synthesis of poly(tetramethylene terephthalate succinate), PTMTS, and poly(tetramethylene terephthalate adipate), PTMTA. The crystal structures of PTMTS and PTMTA were obtained using wide-angle X-ray fiber and powder diffraction data. In an attempt to determine the conformation of these poly(tetramethylene terephthalate dicarboxylates), the infrared spectra of untreated, melted, and cooled PTMTA and PTMTS samples were examined and compared with those of 4GT, PTMS, and PTMA.

Experimental Section

Syntheses. Terephthaloyl chloride, dimethyl terephthalate, and aliphatic diacids (Aldrich Chemical) were used without further purification. Triethylamine or pyridine was refluxed over potassium hydroxide for 2 h and then distilled. Succinoyl chloride and adipoyl chloride (Aldrich Chemical) and ethylene glycol (Fisher Scientific) were distilled. Dichloromethane was also distilled over calcium hydride.

Synthesis of Terephthalates. To synthesize^{33,34} bis(4-hydroxybutyl)terephthalate (BHBT), 15 g of dimethyl terephthalate (0.077 M) and 138.52 g of 1,4-butanediol (1.54 M) along with a few drops of tetraisopropyl titanate(IV) were added to a 250 mL three-necked reaction bottle equipped with a condenser, drying tube, distilling head, and stirrer. The reaction mixture was heated to 160 °C and kept at this temperature for several hours, until all the methanol and tetrahydrofuran formed during the reaction had distilled off. The residue was poured into water and extracted twice with chloroform. The organic extract was washed several times with water until all the unreacted 1,4-butanediol had been removed. It was then dried over anhydrous magnesium sulfate and concentrated. The white product was recrystallized successively from water and from benzene. The yield was 75% (mp, 72 °C; lit. mp 72 °C).

¹H NMR (300 MHz, CDCl₃, ppm): 1.71–1.76 (4H, m), 1.87–1.92 (4H, m), 3.72 (4H, t), 4.38 (4H, t), 8.10 (4H, s).

¹³C NMR (75.4 MHz, CDCl₃, ppm): 25.05, 29.02, 62.18, 65.11, 129.37, 133.94, 165.71.

FTIR (KBr, cm⁻¹): 3415, 2920, 2850, 1720, 1475, 1275, 1130, 1060, 730.

Synthesis of Polymers. The acid chloride synthesis was first undertaken in order to prevent the transreaction of the polyesters. The reaction between BHBT and adipoyl chloride was carried out at room temperature in a dichloromethane solution, using pyridine as an acid acceptor to shift the equilibrium to high molecular weights. Adipoyl chloride (1.16 mL, 0.008 M) was added very slowly to a solution of BHBT (2.50 g, 0.008 M) in dry dichloromethane (150 mL) and pyridine (1.30 mL, 0.016 M). The system was closed, and the mixture was stirred overnight. The molecular weight of the resulting polymer was not high, and fibers could not be drawn. We then operated without solvent and at a higher temperature. The hydrochloric acid generated in the course of the reaction was carried away by a stream of nitrogen. The reaction temperature, between 160 and 180 °C, was maintained for 4 h under atmospheric pressure and for 30 min under low pressure (~0.4 mmHg). The poly(tetramethylene terephthalate dicarboxylates), dissolved in a 50/50 mixture of THF/CH₂Cl₂, were purified by addition of methanol. The nature of the end chain allowed us to evaluate the average molecular weight in number, \bar{M}_n , of the poly(tetramethylene terephthalate dicarboxylates) directly by ¹H NMR in solution in chloroform-*d*. The molecular weights, on the order of 4000, were very low and as such insufficient to anneal the extruded fibers.

In an attempt to obtain higher molecular weights, we raised the reaction temperature to 200 °C and reduced the pressure to ~0.2 mmHg. The analysis of the ¹H NMR spectra showed that the aromatic and aliphatic sequences $[-T-D]_n$ was contaminated by the insertion of $[-T-T]_{-m_1}$ and $[-D-D]_{-m_2}$ fragments. This is probably due to an acidic hydrolysis,

favoring the exchange between the two ester functions. Furthermore, the molecular weights remained low. Thus, the direct esterification of BHBT with dicarboxylic acids, with or without catalyst $\text{Ti}(\text{O}i\text{Pr})_4$, was attempted.

Direct Esterification.^{35–37} **Poly(tetramethylene terephthalate adipate), PTMTA.** An equimolecular mixture of BHBT and adipic acid was used while a stream of nitrogen carried away the water vapor at temperatures over 100 °C. The reaction was first attempted without catalyst at 180 °C and under low pressure. After purification, by precipitation in methanol, the polyester was obtained with a good yields (>75%). The polyester was soluble in the usual organic solvents (CHCl_3 , CH_2Cl_2 , THF, toluene) and insoluble in alcohols or water. Although a regular alternating copolyester was obtained, the molecular weight remained low. A higher molecular weight was obtained at reduced pressure (0.2 mmHg); however, the polyester was contaminated by the presence of homopolymers. The rate of sequence insertion calculated from ^1H and ^{13}C NMR reached 12% for the aromatic sequence, while that of the aliphatic sequence was less than 6%. This is the polymer which was further characterized.

^1H NMR (300 MHz, CDCl_3 , ppm): 1.65–1.67 (4H, m), 1.88–1.96 (8H, m), 2.33 (4H, t), 4.14 (4H, t), 4.37 (4H, t), 8.09 (4H, s).

^{13}C NMR (75.4 MHz, CDCl_3 , ppm): 24.24, 25.14, 25.26, 33.72, 63.70, 64.77, 129.40, 133.89, 165.59, 173.19.

FTIR (KBr, cm^{-1}): 3416, 2961, 2873, 1720, 1716, 1466, 1410, 1271, 1170, 1018, 960, 918, 750.

Anal. Calcd for $\text{C}_{22}\text{H}_{28}\text{O}_8$ considering the regular alternating polymer: C, 63.3; H, 6.8. Calcd according to ^1H NMR results (12% T–T, 6% D–D): C, 63.7; H, 7.0. Found: C, 63.2; H, 7.1.

In another attempt (180 °C, reduced pressure (0.2 mmHg), and $\text{Ti}(\text{O}i\text{Pr})_4$ catalyst) a very brittle polymer, which could not be processed into fibers, was obtained.

Poly(tetramethylene terephthalate succinate), PTMTS. The direct esterification of BHBT and succinic acid was carried out as above. The polyester was purified in the same manner as PTMTA and yielded 75% PTMTS.

^1H NMR (300 MHz, CDCl_3 , ppm): 1.80–1.90 (4H, m), 2.63 (4H, s), 4.16 (4H, t), 4.36 (4H, t), 8.08 (4H, s).

^{13}C NMR (75.4 MHz, CDCl_3 , ppm): 25.14, 25.26, 28.89, 64.05, 64.74, 129.41, 133.89, 165.58, 172.19.

FTIR (KBr, cm^{-1}): 3420, 2960, 2870, 1720, 1716, 1464, 1410, 1271, 1171, 1018, 960, 918, 750.

Anal. Calcd for $\text{C}_{20}\text{H}_{24}\text{O}_8$ considering the regular alternating polymer: C, 61.7; H, 6.1. Calcd according to ^1H NMR results (12% T–T, 6% D–D): C, 62.3; H, 6.3. Found: C, 61.8; H, 6.4.

The different triad sequences, aromatic–aromatic, aromatic–aliphatic, and aliphatic–aliphatic could be distinguished due to the different chemical shifts of the aromatic quaternary carbons of the terephthalate and the CH_2 groups next to the aliphatic carbonyl carbons.

These polymerizations were conducted at much lower temperature than general industrial polycondensation and copolycondensation temperatures of BHET and BHBT i.e., at 180 °C rather than 280–300 °C. Under the conditions of temperature and pressure described above, the ^1H and ^{13}C NMR, analyses show that the percentage of sequence insertion aromatic and aliphatic decreased as the length of the glycol chain increased. In the poly(tetramethylene terephthalate dicarboxylates) the rate of sequence insertion reached 12% for the aromatic sequence, while that of the aliphatic sequences was less than 6%. Under the same conditions, poly(hexamethylene terephthalate dicarboxylates) have a high degree of alternation (99%). However, the rate of aromatic and aliphatic sequence insertion reached 35% for poly(ethylene terephthalate dicarboxylates) and poly(trimethylene terephthalate dicarboxylates).

All infrared spectra were recorded using a Perkin-Elmer FTIR spectrometer. To achieve a high signal-to-noise ratio and at the same time to maximize peak resolution, all spectra were signal averaged with 100 scans at a resolution of 2 cm^{-1} . A specially built thermocell was used to obtain the melt spectra of the polyesters at a temperature approximately 10 °C above their respective melting points.

Table 1. Physical Characteristics of PTMTS and PTMTA

| | PTMTS | PTMTA |
|---------------------------------------|---|---|
| formula | $-\text{[C}_{20}\text{H}_{24}\text{O}_8\text{]}_n-$ | $-\text{[C}_{22}\text{H}_{28}\text{O}_8\text{]}_n-$ |
| fw | 392.40 | 420.46 |
| mol wt | | |
| \bar{M}_n | 6191 | 6514 |
| \bar{M}_w | 16188 | 17177 |
| \bar{M}_z | 29463 | 30214 |
| \bar{M}_w/\bar{M}_n | 2.6 | 2.6 |
| \bar{M}_w/\bar{M}_n | 1.8 | 1.8 |
| density, exptl (g cm^{-3}) | 1.164 | 1.183 |
| density, calcd (g cm^{-3}) | 1.249 | 1.262 |
| mp (°C) | 122–124 | 104–108 |

The density of the amorphous polymers was established by the flotation method in an aqueous solution of ZnCl_2 and measured by picnometry. The melting points were obtained using the TA Instrument DSC 2910 differential scanning calorimeter, with a heating/cooling rate of 10 °C/min.

The polymers' molecular weight distributions were established by gel permeation chromatography using the Waters Co., model Waters R401, chromatograph using THF as eluent at 33 °C. Three Ultrastaygel columns with minimum porosities of 10^3 , 10^4 , and 10^5 Å were mounted in series and kept at 30 °C. The rate of flow of the eluent (THF) was 1 mL min^{-1} . The system was calibrated with narrow-distribution polystyrene. The physical characteristics of the PTMTS and the PTMTA are compared in Table 1.

Structure Determination of PTMTS and PTMTA. The polymers synthesized by the direct esterification procedure at 180 °C and reduced pressure were melt-extruded, and the fibers were annealed under tension for 4 h at 80 and 65 °C for the succinate and the adipate, respectively, and stretched in a screw specimen holder. The diffraction patterns were recorded with Ni-filtered Cu K α radiation in a Laue or a Weissenberg (57.3 mm diameter) camera. The sample-to-film distance was calibrated using NaF powder. The X-ray powder patterns were recorded with a Debye–Scherrer camera, 114.6 mm in diameter.

The unit-cell dimensions of PTMTA and PTMTS were obtained by a trial and error method using all the observed reflection spots recorded on the fiber patterns. The X-ray fiber diffraction patterns of PTMTS and PTMTA are very reminiscent of that of 4GT in the relaxed form. The indexing of the diffraction spots was derived from that of the relaxed form of 4GT. The unit-cell parameters were refined by minimizing the sum of the differences between the squares of the observed and calculated d values (Table 2). The unit-cell dimensions and other crystal data of interest of PTMTS and PTMTA are compared, in Table 3 with the corresponding quantities in 4GT, PTMS,^{29,31} and PTMA.³²

Comparison of the density calculated from the unit-cell dimensions with the experimental value confirmed that there is only one chemical unit per cell. The atomic numbering systems used for PTMTS and PTMTA are illustrated in Figure 1. The structure was assumed to be centrosymmetric about the center of the terephthaloyl group and the midpoint of the central CH_2 – CH_2 bond in the diacid moiety, since this feature is observed in many polyesters that crystallize in the triclinic system, space group $P1$. To build an initial monomer chain, structural data derived from previous X-ray diffraction studies, such as studies on tetramethylene glycol dibenzoate derivatives,³⁸ 4GT, or PTMS, were used. The calculated values of the fiber repeat in the fully extended conformation, would be $p_{c,t} = 25.51$ and 27.96 Å for PTMTS and PTMTA, respectively. Where discrepancies between the various values exist, we have taken the corresponding quantities from dibenzoate derivatives, which are the most relevant to our work. The chains are built so that the calculated fiber repeats match the experimental quantities, $p_o = 23.64$ and 25.05 Å for PTMTS and PTMTA, respectively. Our choices of bond distances and angles for the new polyesters are given in Table 4.

The intensities of the reflection spots were visually estimated on a scale of 0–100 by 20 observers and averaged. The

Table 2. Comparison of Observed and Calculated *d* spacings (Å) of PTMTS and PTMTA

| spot | PTMTA | | | PTMTS | | |
|------|--------------|-------------------------|-------------------------|--------------|-------------------------|-------------------------|
| | <i>h k l</i> | <i>d</i> _{obs} | <i>d</i> _{cal} | <i>h k l</i> | <i>d</i> _{obs} | <i>d</i> _{cal} |
| 1 | 0 1 0 | 5.07 | 5.058 | 0 1 0 | 5.07 | 5.073 |
| 2 | -1 1 0 | 4.17 | 4.162 | -1 1 0 | 4.17 | 4.187 |
| 3 | 1 0 0 | 3.80 | 3.830 | 1 0 0 | 3.80 | 3.773 |
| 4 | -1 2 0 | 2.84 | 2.823 | -1 2 0 | 2.84 | 2.868 |
| 5 | 0 2 0 | 2.53 | 2.529 | 0 2 0 | 2.53 | 2.536 |
| | 1 1 0 | | 2.526 | 1 1 0 | | 2.491 |
| 6 | 0 0 2 | 10.11 | 10.126 | 0 0 2 | 9.61 | 9.607 |
| 7 | 0 -1 2 | 5.55 | 5.566 | 0 -1 2 | 5.54 | 5.519 |
| 8 | -1 1 2 | 4.27 | 4.261 | -1 1 2 | 4.33 | 4.315 |
| 9 | 0 1 2 | 3.87 | 3.910 | 0 1 2 | 3.87 | 3.876 |
| 10 | 1 -1 2 | 3.55 | 3.538 | 1 -1 2 | 3.50 | 3.491 |
| 11 | 1 0 2 | 3.06 | 3.059 | 1 0 2 | 2.97 | 2.986 |
| 12 | 1 1 -2 | 2.78 | 2.875 | | | |
| | 1 -2 2 | | 2.762 | 1 -2 2 | 2.76 | 2.776 |
| | 0 -2 2 | | 2.742 | 0 -2 2 | | 2.747 |
| | | | | -1 2 2 | | 2.721 |
| 13 | 0 0 4 | 5.07 | 5.063 | 0 0 4 | 4.78 | 4.803 |
| 14 | -1 1 4 | 3.79 | 3.729 | -1 1 4 | 3.71 | 3.726 |
| 15 | 1 1 -4 | 3.04 | 3.090 | | | |
| | 0 1 4 | | 2.999 | | | |
| 16 | 1 -1 4 | 2.80 | 2.868 | 1 -1 4 | 2.75 | 2.787 |
| | 0 -2 4 | | 2.783 | 0 -2 4 | | 2.759 |
| 17 | 1 -2 4 | 2.53 | 2.530 | 1 -2 4 | 2.49 | 2.504 |
| 18 | 1 0 4 | 2.47 | 2.461 | | | |
| | 2 1 4 | | 2.432 | | | |
| | | | | -2 1 4 | 2.42 | 2.435 |
| | | | | -1 2 4 | | 2.423 |
| 19 | 0 -1 6 | 3.56 | 3.600 | 0 -1 6 | 3.43 | 3.414 |
| 20 | 1 -1 6 | 2.34 | 2.431 | | | |
| | 2 0 -6 | | 2.315 | | | |
| 21 | 1 0 -8 | 3.08 | 3.038 | 1 0 -7 | 3.24 | 3.256 |
| 22 | 0 -1 8 | 2.77 | 2.786 | 1 1 -7 | 2.80 | 2.815 |
| | 1 1 -8 | | 2.766 | | | |
| 23 | 0 0 8 | 2.51 | 2.532 | 0 0 7 | 2.76 | 2.745 |

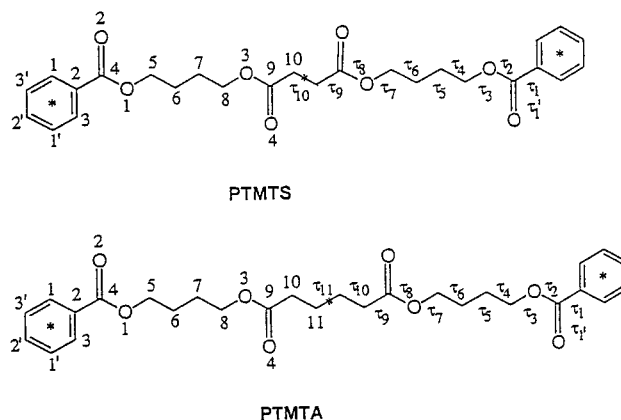
Table 3. Comparison of the Unit Cell Dimensions of the New Polyesters PTMTS and PTMTA to Those of 4GT, PTMS, and PTMA

| | <i>a</i> (Å) | <i>b</i> (Å) | <i>c</i> (Å) | α (deg) | β (deg) | γ (deg) | <i>Z</i> | ref |
|----------------|-----------------|-----------------|-----------------|-------------------|------------------|-------------------|----------|----------|
| PTMTS | 4.89 | 5.95 | 23.64 | 100.4 | 116.9 | 110.7 | 1 | <i>a</i> |
| PTMTA | 4.89 | 5.90 | 25.05 | 102.3 | 116.8 | 108.8 | 1 | <i>a</i> |
| α -4GT | 4.83 | 5.96 | 11.62 | 99.9 | 115.2 | 111.3 | 1 | 3 |
| | 4.8(9) | 5.9(5) | 11.6(7) | 98.0 | 116.0 | 110.0 | 1 | 6 |
| β -4GT | 4.95 | 5.67 | 12.95 | 101.7 | 121.8 | 99.9 | 1 | 5 |
| | 4.70 | 5.80 | 13.00 | 102.0 | 121.0 | 105.0 | 1 | 6 |
| α -PTMS | 5.23 | 9.08 | 10.80 | 90 | 123.9 | 90 | 2 | 9, 20 |
| β -PTMS | | | 11.97 | | | | 2 | 20 |
| α -PTMA | 6.69 | 8.00 | 14.20 | 90 | 45.5 | 90 | 2 | 22 |
| β -PTMA | 5.05 | 7.36 | 14.65 | 90 | 90 | 90 | 2 | 22 |

^a This work.

observed structure factors, $|F_o|$'s, were derived after the Lorentz and polarization corrections were applied. The intensity attributed to unobserved reflections was half that of the lowest observed value. The polymer chain was placed in the unit cell so that the center of the terephthaloyl group and the midpoint of the aliphatic acid coincide with the crystallographic centers of symmetry of the unit cell. The bond lengths and angles were kept constant, at the values given in Table 4, while the torsion angles τ_3 , τ_4 , τ_6 , and τ_7 (glycol segment) and torsion angles τ_8 and τ_9 (diacid segment), defined in Figure 1, were allowed to vary in order to find the most probable conformation for PTMTS and for PTMTA. The X-ray fiber pattern was computed using the Cerius² software and compared to its experimental counterpart (Figure 2).

Packing energies were minimized using the Cerius² program release 1.6 package. The Dreiding force field³⁹ and the Polak-Ribiere conjugate gradient technique⁴⁰ were employed. During this minimization the polyester chains, which were considered as rigid units to preserve the crystallographic restraints, were

**Figure 1.** Schematic representation and atomic numbering of PTMTS and PTMTA.**Table 4. Bond Distances and Angles Adopted in the Present Work for PTMTS and PTMTA**

| distances (Å) | | angles (deg) | |
|---------------|-------|--------------------|-------|
| C(1)–C(2) | 1.404 | C(3')–C(1)–C(2) | 120.4 |
| C(1)–C(3') | 1.408 | C(2)–C(3)–H(3) | 120.2 |
| C(2)–C(3) | 1.408 | C(2)–C(3)–C(1') | 120.2 |
| C(2)–C(4) | 1.48 | C(1')–C(3)–H(3) | 119.5 |
| C(4)–O(1) | 1.34 | C(1)–C(2)–C(4) | 118 |
| C(4)–O(2) | 1.20 | C(1)–C(2)–C(3) | 119.4 |
| O(1)–C(5) | 1.45 | C(3)–C(2)–C(4) | 122.6 |
| C(5)–C(6) | 1.52 | C(2)–C(4)–O(2) | 124 |
| C(6)–C(7) | 1.53 | C(2)–C(1)–O(1) | 119 |
| C(7)–C(8) | 1.52 | O(2)–C(4)–O(1) | 117 |
| C(8)–O(3) | 1.45 | C(4)–O(1)–C(5) | 116 |
| O(3)–C(9) | 1.34 | O(1)–C(5)–C(6) | 109.5 |
| C(9)–O(4) | 1.20 | C(5)–C(6)–C(7) | 113 |
| C(9)–C(10) | 1.49 | C(6)–C(7)–C(8) | 113 |
| C(10)–C(11) | 1.52 | C(7)–C(8)–O(3) | 109.5 |
| C(11)–C(12) | 1.50 | C(8)–O(3)–C(9) | 114 |
| | | O(3)–C(9)–O(4) | 122.9 |
| | | O(3)–C(9)–C(10) | 113 |
| | | O(4)–C(9)–C(10) | 124 |
| | | C(9)–C(10)–C(11) | 111 |
| | | C(10)–C(11)–C(11') | 103 |

rotated within the unit cell around the *c* axis.

The calculated structure factors, $|F_c|$'s, were obtained from the model chain in its best orientation in the unit cell and compared to the corresponding $|F_o|$ values. To improve the agreement between the observed and calculated structure factors, some slight conformational changes were made and minor modifications of the torsion angles were also examined so that the length of the fiber repeat and the *c* dimension coincided exactly. The refinement process was based on minimizing the quantity $\Delta = \sum w(|F_o| - |F_c|)^2$, where *w* is a weighting coefficient assigned from the observed diffracted intensities. Unobserved reflections were included at the threshold intensity and only omitted from the refinement if the calculated value was less than this. The scattering factors for the oxygen and carbon atoms were taken from Cromer and Mann⁴¹ and those for H atoms from Stewart, Davidson, and Simpson.⁴²

Results and Discussion

Nuclear Magnetic Resonance. The confirmation of the integrity of the chemical repeat of the polyesters was established by proton and ¹³C NMR in deuterated chloroform solution. The ¹H NMR spectra recorded for the poly(tetramethylene terephthalate dicarboxylates) are shown in Figure 3 and the assignment of the peaks was confirmed by the assignments made for the model compounds,⁴³ those of 4GT,⁴⁴ and those of the corresponding aliphatic polyesters.⁴⁵ The two methylenic protons of the tetramethylene segment next to the O

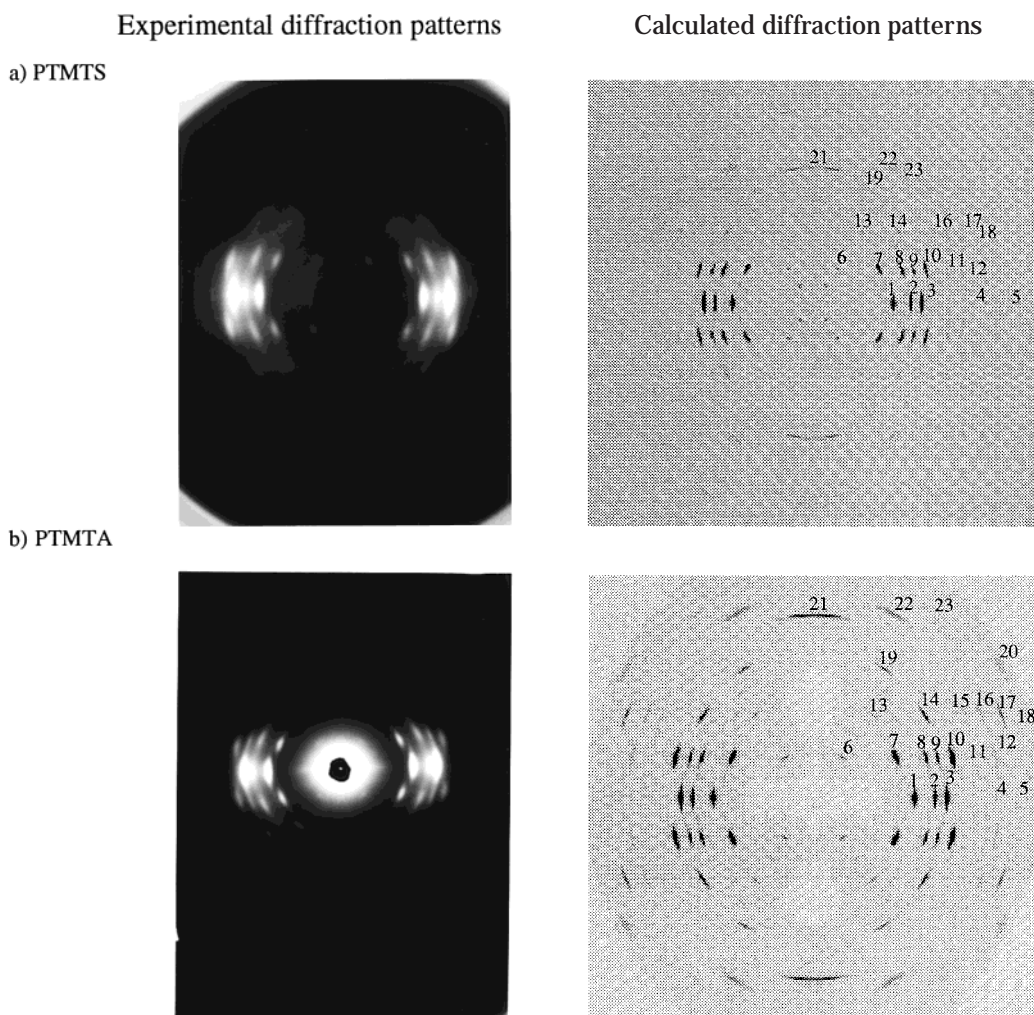


Figure 2. Experimental and calculated X-ray diffraction patterns of PTMST and PTMTA.

atoms are not chemically equivalent, since one of them is surrounded by CO (aromatic) and methylenic protons, while the other is surrounded by CO (aliphatic) and methylenic protons. Thus, there is no symmetry in this segment and two resonance peaks of $-\text{OCH}_2-$ occur in these structures at 4.14 and 4.36 ppm. There is an extra peak (singlet at 2.63 ppm), indicating the presence of the succinate's protons, while a triplet near 2.33 ppm is observed in the adipate. Additional peaks, (multiplet) are also observed in addition to those in PTMST. These resonance peaks are indicative of their environment and are sufficient to characterize and quantify changes in the chain length of these polyesters.

The ^{13}C NMR spectra of the polyesters are shown in Figure 4. There are two kinds of ^{13}C carbonyl chemical shifts: the aromatic and the aliphatic carbonyl, observed with the same intensity at 165.5 and 173.1 ppm, respectively. The two resonance peaks near 64.05 and 64.77 ppm suggest the presence of nonequivalent CH_2 groups in close proximity to the O atoms. The same phenomenon was observed for the two nonequivalent central CH_2-CH_2 groups of the glycolic sequence (25.26 and 25.14 ppm). The signals observed in the alkyl region, in particular the peaks at 28.89 and 33.72 ppm, are attributed to the CH_2 groups next to the aliphatic carbonyl carbons in PTMST and PTMTA, respectively.

Infrared spectroscopy. The determination of the conformation around the $\text{O}-\text{CH}_2$ and CH_2-CH_2 bonds

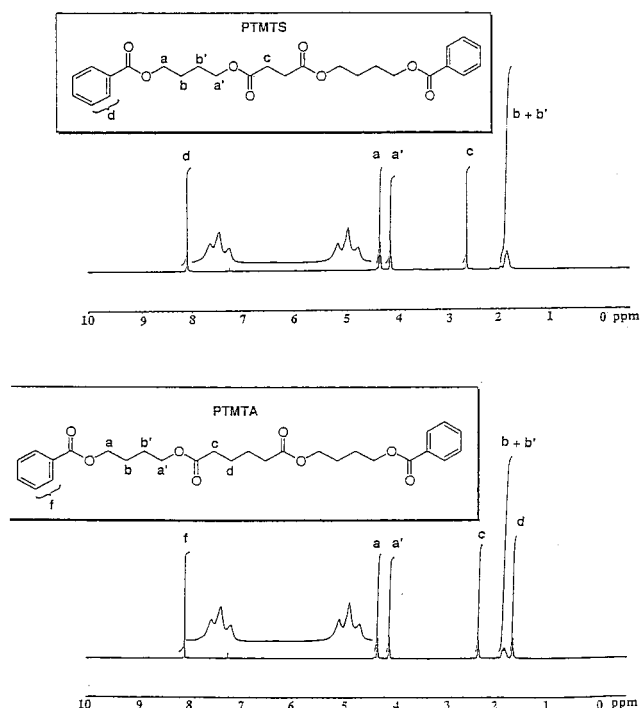


Figure 3. ^1H NMR spectra of PTMST and PTMTA.

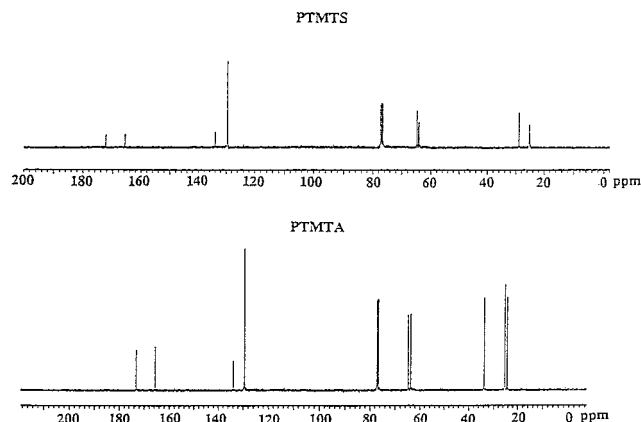


Figure 4. The ^{13}C NMR spectra of PTMTS and PTMTA.

of poly(tetramethylene terephthalate dicarboxylates) were investigated by infrared spectroscopy. We report here the infrared spectra of untreated and melted poly(tetramethylene terephthalate dicarboxylates) and their comparison to the dynamic infrared spectra of 4GT^{19–23} and PTMS.³¹

In the range of the most sensitive bands, as noted in the published infrared spectra of the poly(*n*-methylene terephthalates),¹⁷ the infrared spectra of the untreated PTMTS and PTMTA, reproduced in Figure 5a, show great similarity and can be discussed along the same lines as the spectrum of 4GT. It has been reported⁴⁵ that centrosymmetric molecules display a strong and sharp single C=O stretching band at about 1715 cm^{-1} , while in the noncentrosymmetric cases this band is usually split into two very close bands, 5 cm^{-1} apart. However, here the two C=O absorptions, observed at 1730 and 1717 cm^{-1} , are attributed to the two chemically different C=O groups. The aromatic ring modes can be assigned to the bands at 1580 , 1505 , 1410 , 1015 , and 870 cm^{-1} .

However, the major differences in the FTIR spectra are observed in the region of the methylene modes. The band at 917 cm^{-1} in α -4GT, was assigned^{19–23} to the C–H rocking modes of the nongauche–nontrans $\text{CH}_2\text{--CH}_2$ structure proposed by Mencik¹³ and Pass and Hall¹⁶ in their X-ray structure determinations. The relative intensities of the two bands at 938 (s) and 960 cm^{-1} (m) in α -4GT form are interchanged upon stretching the specimen to the β -form. It was also reported that the band at 750 cm^{-1} is characteristic of the α -form.

The FTIR spectra of PTMS under various strains have been reported by Ichikawa et al.³¹ The intensities of the peaks at 955 and 920 cm^{-1} start decreasing at a strain of about 8%, while a new band appears at 977 cm^{-1} . These observations thus indicate that the bands at 955 and 920 cm^{-1} characterize the α -form, while the band at 977 cm^{-1} is assigned to the β -form.

We recorded and examined the infrared spectra of PTMA in which the two methylenic sequences (glycol and acid) are in an all-trans conformation; the 930 (more intense) and 960 cm^{-1} bands are present.

In our case, the 917 and 749 cm^{-1} bands appear in the infrared spectra of the bulk polymers. The same phenomenon is observed for the bands at 958 and 940 cm^{-1} (more intense), and its relative intensities are comparable to those observed in the amorphous state of 4GT. This observation indicates that the untreated polymers probably contain the two phases found in 4GT and in PTMS.

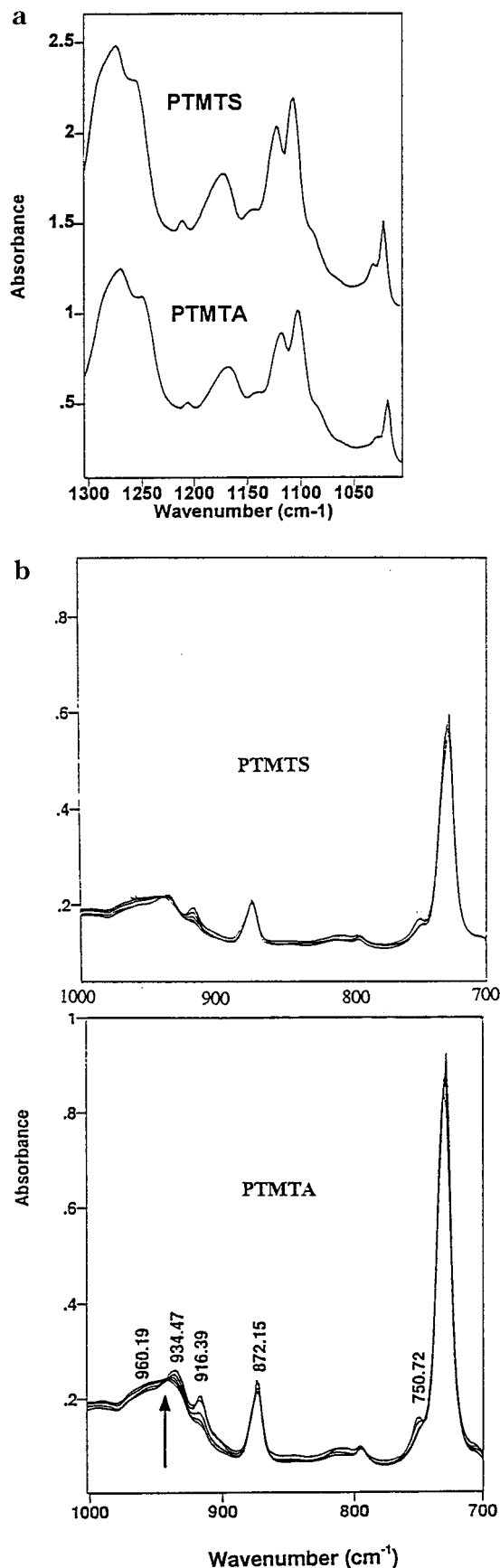
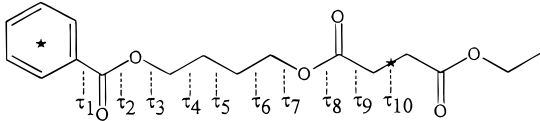


Figure 5. (a) The $1000\text{--}1300\text{ cm}^{-1}$ region of the FTIR spectra of the poly(tetramethylene terephthalate dicarboxylates) at room temperature. (b) The $700\text{--}1000\text{ cm}^{-1}$ region of the dynamic FTIR of PTMTS and PTMTA.

Table 5. Variation of the Calculated Fiber Repeat of PTMTS, p_c , with the Torsion Angles^a


| | τ_1 | τ_2 | τ_3 | τ_4 | τ_5 | τ_6 | τ_7 | τ_8 | τ_9 | τ_{10} | $p_c, \text{\AA}$ |
|------|----------|----------|----------|----------|----------|----------|----------|----------|----------|-------------|--------------------|
| I | | | 90 | | | | | | | | 24.40 ^b |
| II | | | | | | | 90 | | | | 23.05 ^b |
| III | | | 90 | | | | 90 | | | | 22.65 |
| IV | | | 90 | | | | -90 | | | | 23.90 ^b |
| V | | | -90 | | | | 90 | | | | 23.45 ^b |
| VI | | | 90 | 90 | | | | | | | 21.75 |
| VII | | | -90 | 90 | | | | | | | 21.53 |
| VIII | | | 90 | -90 | | | | | | | 19.65 |
| IX | | | 90 | 90 | | -90 | -90 | | | | 23.15 ^b |
| X | | | | | | 90 | 90 | | | | 22.25 |
| XI | | | | | | -90 | 90 | | | | 18.15 |
| XII | | | | | | | | 60 | | | 20.60 |
| XIII | | | | | | | | 90 | | | 22.25 |
| XIV | | | | | | | | 120 | | | 23.75 ^b |

^a Only the torsion angles different from 180° were indicated.^b The calculated fiber repeat must be close to the experimental value, $p_{\text{exp}} = 23.64 \text{ \AA}$.

In the bending region, the relatively weak bands at 1322 and 1350 cm^{-1} observed in α -4GT decrease in intensity when stress¹⁸ is applied. They almost disappear in the β -phase. These bands are present in the four poly(tetramethylene terephthalate dicarboxylates) that we synthesized and resemble those found in the α -phase. We note that they are absent from the infrared spectra of PTMA. The bands at 1390 and 1410 cm^{-1} in α -4GT, assigned to the $-\text{CH}_2$ bending mode^{18,20} associated with the two methylene groups adjacent to the central trans bond of the tetramethylene sequence, are also present in all infrared spectra of poly(tetramethylene terephthalate dicarboxylates).

To clarify this situation, a dynamic FTIR study was undertaken. Heating and cooling produce few spectral changes (Figure 5b). Upon heating, the intensities of the 749.5, 940.3, and 917.8 cm^{-1} bands for the PTMTS and those at 748.5, 936.5, and 916.6 cm^{-1} for the PTMTA decrease while the intensities of the bands at 957.8 cm^{-1} for the PTMTS and at 959.0 cm^{-1} for the PTMTA increase. An isosbestic point is noted at 947 cm^{-1} . According to Siesler,²² Tashiro et al.,²³ and Ichikawa et al.,³¹ the existence of such an isosbestic point indicates that the crystal transition occurred only between the

α - and the β -form, where no amorphous part is transformed into crystal. The broad peak at about 990 cm^{-1} in samples of 4GT quenched from the melt (i.e., highly amorphous) is analogous to the peak observed in the melt spectra of PTMTS and PTMTA (Figure 5b), and no absorbance peak characteristic of the α -form was observed. Upon cooling, the intensities of the characteristic absorbance peaks of the α -form increase while the intensity of the characteristic bands of the β -form decrease, indicating that the transition is reversible and that the α -form is the more stable structure at room temperature. Consequently, the similarity of the crystal transition mechanism and the infrared spectra of 4GT, PTMS, and poly(tetramethylene terephthalate dicarboxylates) suggests that the conformation of the glycolic sequence associated with these polyesters is the same.

X-ray Diffraction Study. Chain Conformation.

By taking into account the spectroscopic considerations (NMR and FTIR) and the experimental value of the fiber repeat, several models were built using the bond distances and angles derived from the crystallographic studies of a number of dibenzoates.³⁸ These models must satisfy the conditions stated below:

- (1) The calculated fiber repeat must be close to the experimental value.
- (2) The nontrans nongauche torsion angles should be localized in the tetramethylene glycol segment.
- (3) The possibility of slight distortions in the adipate segment must be considered.
- (4) The succinate segment should be in the all-trans conformation.

For PTMTS, the values of the fiber repeat calculated from the models having at least one nontrans-nongauche, $\text{O}-\text{CH}_2$, torsion angle are given in Table 5. By comparing these values with the observed fiber repeat, $p_0 = 23.64 \text{ \AA}$, only models I, II, IV, V, IX, and XIV are retained. Conformation XIV does not explain the presence of the absorption band at 917 cm^{-1} in the infrared spectra of the poly(tetramethylene terephthalate dicarboxylates). This model is therefore rejected. To match the calculated and observed fiber repeats, the torsion angles τ_3 , τ_4 , τ_6 , and τ_7 of the glycol segment have been varied between 90 and 150°, whereas in the diacid portion, the torsion angles τ_8 and τ_9 have been subjected to some variations around 180°.

In models I and II, the conformation of the tetramethylene glycol segments are respectively stttt or s⁻tttt, and tttts or tttts⁻. Despite the different combina-

Table 6. Variation of the Agreement Index, R_w , with the Torsion Angles in PTMTS and PTMTA ($B = 13.7 \text{ \AA}^2$), Where in Both Cases the Chosen Conformation Is No. 4^a

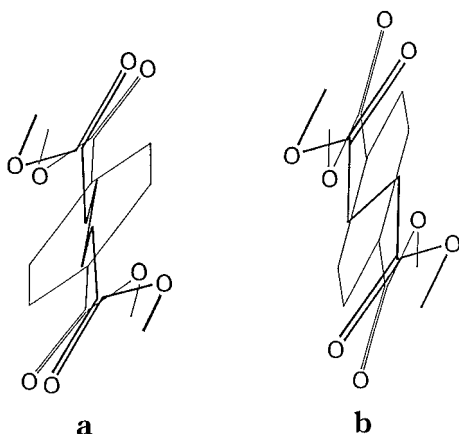
| | PTMTS | | | | PTMTA | | | |
|---|--------|--------|--------|--------|-------|--------|--------|--------|
| | 1 | 2 | 3 | 4 | 1 | 2 | 3 | 4 |
| $\tau_1 = \text{C}(1)-\text{C}(2)-\text{C}(4)-\text{O}(1)$ | 178.1 | 178.1 | 179.2 | 179.2 | 179.2 | 179.2 | 178.7 | 178.4 |
| $\tau_1' = \text{C}(1)-\text{C}(2)-\text{C}(4)-\text{O}(2)$ | -1.2 | -1.2 | -0.9 | -0.8 | -1.1 | -0.8 | -0.8 | -0.8 |
| $\tau_2 = \text{C}(2)-\text{C}(4)-\text{O}(1)-\text{C}(5)$ | 173.5 | 173.5 | 175.2 | 176.3 | 175.2 | 175.2 | 176.7 | 176.3 |
| $\tau_3 = \text{C}(4)-\text{O}(1)-\text{C}(5)-\text{C}(6)$ | -116.2 | -117.5 | -117.5 | -118 | -94.3 | -95.6 | -95.6 | -97 |
| $\tau_4 = \text{O}(1)-\text{C}(5)-\text{C}(6)-\text{C}(7)$ | -112.5 | -117.5 | -117.5 | -118 | -93.1 | -91.6 | -91.6 | -90 |
| $\tau_5 = \text{C}(5)-\text{C}(6)-\text{C}(7)-\text{C}(8)$ | -179.3 | -179 | -179 | -179 | -179 | -178.8 | -178.8 | -179 |
| $\tau_6 = \text{C}(6)-\text{C}(7)-\text{C}(8)-\text{O}(3)$ | 93.3 | 95 | 95 | 96 | 85.7 | 83.2 | 83.2 | 83 |
| $\tau_7 = \text{C}(7)-\text{C}(8)-\text{O}(3)-\text{C}(9)$ | 97.3 | 96.5 | 96.5 | 96 | 91.5 | 92.3 | 92.3 | 90 |
| $\tau_8 = \text{C}(8)-\text{O}(3)-\text{C}(9)-\text{C}(10)$ | -162.5 | -162.5 | -164.2 | -161 | -160 | -160 | -157 | -156.5 |
| $\tau_9 = \text{O}(3)-\text{C}(9)-\text{C}(10)-\text{C}(11)$ | -169.5 | -169.5 | -170.2 | -167.5 | -147 | -147 | -142 | -141 |
| $\tau_{10} = \text{C}(9)-\text{C}(10)-\text{C}(11)-\text{C}(11')$ | 180 | 180 | 180 | 180 | 167.5 | 167.5 | 169.0 | 169.5 |
| $\tau_{11} = \text{C}(10)-\text{C}(11)-\text{C}(11')-\text{C}(10')$ | | | | | 180 | 180 | 180 | 180 |
| $R_w, \%$ | 16.8 | 15.7 | 16.0 | 15.3 | 19.9 | 19.6 | 14.6 | 13.5 |
| $E, \text{kcal/mol}$ | -68.5 | -71.7 | -73.1 | -76.4 | -37.3 | -38.7 | -44.5 | -46.7 |

^a The torsion angles and the atomic numbering are given in Figure 1.

Table 7. Comparison of the Conformational Angles of Interest in PTMTS and PTMTA to Those Published for 4GT (1, Mencik; 2, Yokouchi et al.; 3, Hall and Pass; 4, Desborough and Hall)^a

| | α -4GT | | | | this work | |
|--|---------------|-------|--------|--------|-----------|--------|
| | 1 | 2 | 3 | 4 | PTMTS | PTMTA |
| $\tau_1 = \text{C}(1)\text{--C}(2)\text{--C}(4)\text{--O}(1)$ | 174.8 | 173.8 | 179.2 | 179.2 | 179.2 | 179.2 |
| $\tau_1' = \text{C}(1)\text{--C}(2)\text{--C}(4)\text{--O}(2)$ | -3.5 | 1.8 | -0.6 | -0.8 | -0.8 | -0.8 |
| $\tau_2 = \text{C}(2)\text{--C}(4)\text{--O}(1)\text{--C}(5)$ | 177.5 | 178 | -177.8 | -177.1 | 176.3 | 176.3 |
| $\tau_3 = \text{C}(4)\text{--O}(1)\text{--C}(5)\text{--C}(6)$ | -90.6 | -88 | -94.5 | -92.5 | -118 | -97 |
| $\tau_4 = \text{O}(1)\text{--C}(5)\text{--C}(6)\text{--C}(7)$ | -88.4 | -68 | -79.3 | -76.2 | -118 | -95 |
| $\tau_5 = \text{C}(5)\text{--C}(6)\text{--C}(7)\text{--C}(8)$ | 180 | 180 | 180 | 180 | -179 | -179 |
| $\tau_6 = \text{C}(6)\text{--C}(7)\text{--C}(8)\text{--O}(3)$ | | | | | 96 | 83 |
| $\tau_7 = \text{C}(7)\text{--C}(8)\text{--O}(3)\text{--C}(9)$ | | | | | 96 | 90 |
| $\tau_8 = \text{C}(8)\text{--O}(3)\text{--C}(9)\text{--C}(10)$ | | | | | -161 | -156.5 |
| $\tau_9 = \text{O}(3)\text{--C}(9)\text{--C}(10)\text{--C}(11)$ | | | | | -167.5 | -141 |
| $\tau_{10} = \text{C}(9)\text{--C}(10)\text{--C}(11)\text{--C}(11')$ | | | | | 180 | 169.5 |
| $\tau_{11} = \text{C}(10)\text{--C}(11)\text{--C}(11')\text{--C}(10')$ | | | | | | 180 |

^a The torsion angles and the atomic numbering are given in Figure 1. In cases 1 to 4, the tetramethylene moiety is centrosymmetric. Thus, $\tau_6 = -\tau_4$, $\tau_7 = -\tau_3$, $\tau_8 = -\tau_2$, and $\tau_9 = -\tau_1$.

**Figure 6.** Projection onto the *ab* plane: (a) PTMTS; (b) PTMTA.

tions and adjustments of the torsion angles, the gap between the observed and the calculated fiber repeats remains approximately 0.5 Å. Consequently, these two models were rejected. Only conformations IV and V, comparable with that of PE(4,2), and the conformation IX comparable with that of the α -4GT form, remain possible. In all three cases, the calculated and observed fiber repeats coincide when the torsion angles τ_8 and τ_9 deviate significantly from 180°.

The same protocol has been applied to the PTMTA. The adjustable torsion angles were τ_3 , τ_4 , τ_6 , and τ_7 (glycol segment) and τ_8 , τ_9 , and τ_{10} (adipate segment). The conformations acceptable for the PTMTS have been retained for the PTMTA. This choice is also justified by the similarity between their experimental fiber diagrams and their infrared spectra.

Choice and Confirmation of Chain Conformation. The molecular modeling study followed by the minimization of the packing interactions yielded structures which were selected and then confirmed by a comparison of the observed and calculated fiber diagrams and structure factor calculations. The torsion angles which result in the best match are given in Table 6 where they are compared to the published values for 4GT (α -form).

To choose among conformations IV, V, and IX, and thus establish which is the most favorable arrangement of the PTMTS and PTMTA chains within their unit cell, the fiber diagram is generated, for each conformation and is visually compared to its experimental counterpart.

Table 8. Comparison of the Observed and the Calculated Structure Factors of PTMTA and PTMTS

| spot | PTMTA | | | | PTMTS | | | |
|------|--------------|---------|---------|----------|--------------|---------|---------|----------|
| | <i>h k l</i> | $ F_o $ | $ F_c $ | <i>w</i> | <i>h k l</i> | $ F_o $ | $ F_c $ | <i>w</i> |
| 1 | 0 1 0 | 3.08 | 2.691 | 1.0 | 0 1 0 | 3.43 | 3.173 | 1.0 |
| 2 | -1 1 0 | 2.61 | 2.472 | 1.0 | -1 1 0 | 2.61 | 2.219 | 1.0 |
| 3 | 1 0 0 | 4.62 | 3.701 | 1.0 | 1 0 0 | 4.66 | 3.975 | 1.0 |
| 4 | -1 2 0 | 0.78 | 0.781 | 1.0 | -1 2 0 | 0.55 | 0.370 | 1.0 |
| 5 | 0 2 0 | | 0.234 | | 0 2 0 | | 0.470 | |
| | 1 1 0 | | 0.459 | | 1 1 0 | | 0.409 | |
| | | 0.59 | 0.515 | 0.5 | | 0.59 | 0.623 | 0.5 |
| 6 | 0 0 2 | 0.48 | 0.476 | 1.0 | 0 0 2 | 0.57 | 0.516 | 1.0 |
| 7 | 0 -1 2 | 2.92 | 3.200 | 1.0 | 0 -1 2 | 2.40 | 2.214 | 1.0 |
| 8 | -1 1 2 | 2.39 | 2.322 | 1.0 | -1 1 2 | 2.74 | 2.679 | 1.0 |
| 9 | 0 1 2 | 2.04 | 1.984 | 1.0 | 0 1 2 | 2.05 | 1.877 | 1.0 |
| 10 | 1 -1 2 | 4.05 | 4.188 | 1.0 | 1 -1 2 | 3.45 | 3.423 | 1.0 |
| 11 | 1 0 2 | 0.47 | 0.163 | 0.5 | 1 0 2 | 1.07 | 0.139 | 0.5 |
| 12 | 1 1 -2 | | 0.487 | | | | | |
| | 1 -2 2 | | 1.010 | | 1 -2 2 | | 0.379 | |
| | 0 -2 2 | | 0.510 | | 0 -2 2 | | 0.272 | |
| | | 1.18 | 1.232 | 0.8 | -1 2 2 | | 0.863 | |
| | | | | | | 0.79 | 0.981 | 0.8 |
| 13 | 0 0 4 | 0.84 | 0.697 | 1.0 | 0 0 4 | 0.71 | 0.541 | 1.0 |
| 14 | -1 1 4 | 2.15 | 2.028 | 1.0 | -1 1 4 | 0.94 | 3.726 | 1.0 |
| 15 | 1 1 -4 | | 0.381 | | | | | |
| | | 0.83 | 0.761 | 0.8 | | | | |
| 16 | 1 -1 4 | | 0.185 | | 1 -1 4 | | 1.042 | |
| | 0 -2 4 | | 0.940 | | 0 -2 4 | | 0.460 | |
| | | 0.87 | 0.958 | 0.8 | | 1.11 | 1.139 | 0.8 |
| 17 | 1 -2 4 | 1.82 | 1.895 | 1.0 | 1 -2 4 | 0.84 | 0.886 | 1.0 |
| 18 | 1 0 4 | | 0.517 | | | | | |
| | 2 1 4 | | 0.465 | | | | | |
| | | 0.74 | 0.696 | 0.8 | | | | |
| | | | | | -2 1 4 | | 0.651 | |
| | | | | | -1 2 4 | | 0.314 | |
| | | | | | | 0.61 | 0.723 | 0.8 |
| 19 | 0 -1 6 | 1.07 | 1.061 | 1.0 | 0 -1 6 | 0.70 | 0.614 | 1.0 |
| 20 | 1 -1 6 | | 1.190 | | | | | |
| | 2 0 -6 | | 1.108 | | | | | |
| | | 1.74 | 1.626 | 0.8 | | | | |
| 21 | 1 0 -8 | 1.18 | 1.234 | 1.0 | 1 0 -7 | 0.88 | 0.856 | 1.0 |
| 22 | 0 -1 8 | | 0.924 | | 1 1 -7 | 0.96 | 1.057 | 1.0 |
| | 1 1 -8 | | 1.076 | | | | | |
| | | 1.37 | 1.418 | 1.0 | | | | |
| 23 | 0 0 8 | 0.84 | 0.844 | 1.0 | 0 0 7 | 0.84 | 0.844 | 1.0 |

As mentioned previously, the fiber diagrams of these two polyesters show strong analogies between them and with that of the α -4GT. In both cases, the most intense diffraction spots are found on the *hk0* and *hk2* layers with relatively comparable positions. They are the equatorial reflections, 1 0 0 and 0 1 0, estimated visually to be 100 and 80%, and the reflections 1 -1 2 and 0 -1 2, estimated to be 80 and 70%, respectively.

In the case of PTMTS, the fiber diagrams generated from the most favorable arrangement of the chain in

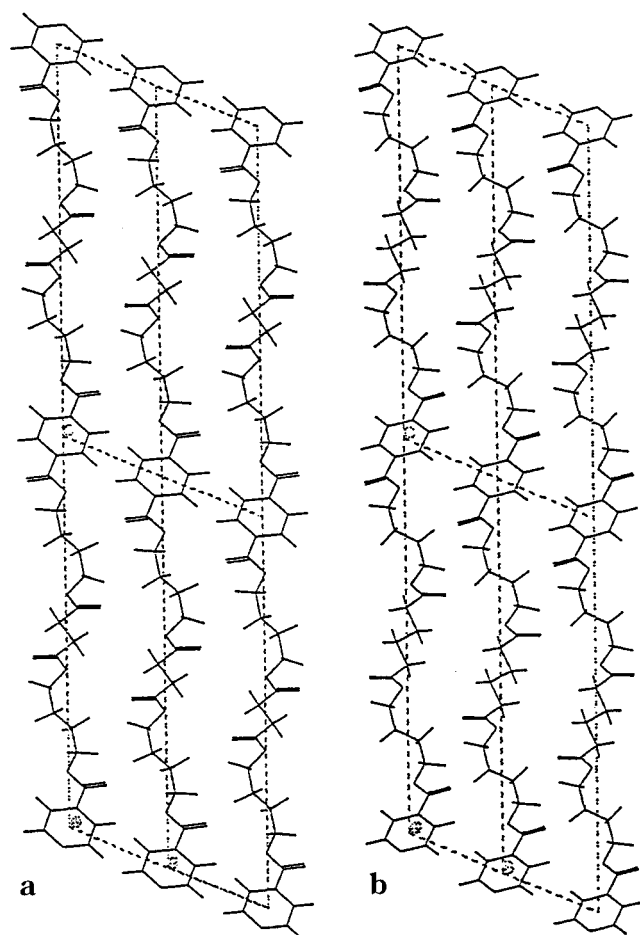


Figure 7. Projection onto the *bc* plane: (a) PTMTS; (b) PTMTA.

conformation IV or V show relatively strong reflections localized on the odd layer lines. Moreover, the equatorial reflection $-1\ 1\ 0$, whose experimental intensity is estimated at 30%, is calculated with a very strong intensity. Furthermore, despite various adjustments of the torsion angles τ_3 and τ_7 , from 90 to 150° , and the torsion angles of the diacidic portion, the intensities of the strong reflections $1\ -1\ 2$ and $0\ -1\ 2$, are always calculated with weak intensities. Finally, the experimentally unobserved reflections localized on the odd layers, especially the $0\ 0\ 1$, $0\ 1\ 1$, $1\ -1\ 1$, $1\ -2\ 1$, $0\ 0\ 3$, $0\ 1\ 3$, and $1\ 1\ -5$ reflections, remain visible and relatively more intense than the observed reflections $0\ 0\ 2$, $-1\ 2\ 0$, and $0\ 2\ 0$ or $1\ 1\ 0$. Consequently, the conformations IV and V are rejected. Only model IX, in which the glycolic sequence has a conformation comparable to that of the α -4GT form, describes correctly the structure of the poly(tetramethylene terephthalate succinate). Indeed, the fiber diagram generated with the PTMTS chains in conformation IX reproduces the relative order of the intensities of the equatorial reflections. The nongauche-nontrans torsion angles τ_3 and τ_4 have values of about 118° , and τ_6 and τ_7 are near 96° . The variation of the τ_4 and τ_7 torsion angles affects strongly the equatorial reflection intensity, in particular the $1\ 0\ 0$ reflection. The intensities of the odd layer-line reflections ($l = 1$ and 3), especially $0\ 0\ 1$, $0\ 1\ 1$, and $0\ 0\ 3$ decrease when the succinate torsion angles deviate from 180° and reach 2–3% when $\tau_8 = -161^\circ$. The intensities of the reflections on the second and fourth layer lines, especially $1\ -1\ 2$ and $0\ 1\ 2$, become optimal when the

Table 9. Fractional Atomic Coordinates of PTMTS and PTMTA

| atom | <i>x/a</i> | <i>y/b</i> | <i>z/c</i> |
|--------|------------|------------|------------|
| PTMTS | | | |
| C(1) | 0.09792 | 0.26117 | 0.03380 |
| C(2) | -0.02153 | 0.07274 | 0.05750 |
| C(3) | -0.11845 | -0.18847 | 0.02366 |
| C(4) | -0.04048 | 0.16025 | 0.11775 |
| O(1) | -0.15583 | -0.01663 | 0.14095 |
| O(2) | 0.04508 | 0.38319 | 0.14824 |
| C(5) | -0.14688 | 0.08310 | 0.20102 |
| C(6) | 0.10084 | 0.03638 | 0.25940 |
| C(7) | -0.10721 | -0.14249 | 0.28072 |
| C(8) | 0.14052 | -0.18922 | 0.33910 |
| C(9) | 0.06431 | -0.11180 | 0.42846 |
| O(3) | 0.25534 | -0.01080 | 0.40375 |
| O(4) | -0.12666 | -0.34603 | 0.40322 |
| C(10) | 0.07948 | 0.07100 | 0.48348 |
| H(1) | 0.17490 | 0.46521 | 0.05975 |
| H(3) | 0.21079 | 0.33686 | 0.04154 |
| H(5) | -0.41059 | -0.01595 | 0.19066 |
| H(15) | -0.05088 | 0.29436 | 0.21880 |
| H(6) | 0.31279 | 0.21764 | 0.30584 |
| H(16) | 0.21698 | -0.06554 | 0.24331 |
| H(7) | -0.32046 | -0.33611 | 0.23911 |
| H(17) | -0.21558 | -0.04958 | 0.30210 |
| H(8) | 0.00618 | -0.38962 | 0.33399 |
| H(18) | 0.37600 | -0.15731 | 0.33963 |
| H(10) | 0.35950 | 0.21664 | 0.52097 |
| H(110) | -0.06346 | 0.16456 | 0.45736 |
| PTMTA | | | |
| C(1) | 0.21439 | 0.26840 | 0.04337 |
| C(2) | 0.00610 | 0.09871 | 0.05727 |
| C(3) | -0.20902 | -0.16981 | 0.01364 |
| C(4) | 0.02494 | 0.21318 | 0.11822 |
| O(1) | -0.17783 | 0.05618 | 0.13164 |
| O(2) | 0.21011 | 0.44157 | 0.15685 |
| C(5) | -0.13014 | 0.17758 | 0.19410 |
| C(6) | 0.11302 | 0.11538 | 0.24554 |
| C(7) | -0.08036 | -0.13938 | 0.24819 |
| C(8) | 0.16224 | -0.19904 | 0.30046 |
| C(9) | 0.01441 | -0.17986 | 0.37748 |
| O(3) | 0.23865 | -0.05121 | 0.36408 |
| O(4) | -0.14350 | -0.41657 | 0.35463 |
| C(10) | 0.00089 | 0.00093 | 0.42668 |
| C(11) | -0.02985 | -0.11349 | 0.47386 |
| H(1) | 0.38239 | 0.47785 | 0.07682 |
| H(3) | -0.37290 | -0.30390 | 0.02365 |
| H(5) | -0.01527 | 0.39152 | 0.21116 |
| H(15) | -0.37693 | 0.10346 | 0.19004 |
| H(6) | 0.25420 | 0.26498 | 0.29572 |
| H(16) | 0.29975 | 0.08588 | 0.23648 |
| H(7) | -0.27328 | -0.13287 | 0.25824 |
| H(17) | -0.21152 | -0.30610 | 0.20108 |
| H(8) | 0.04503 | -0.40742 | 0.29046 |
| H(18) | 0.40808 | -0.14305 | 0.30436 |
| H(10) | -0.22429 | 0.02800 | 0.39924 |
| H(110) | 0.24021 | 0.18888 | 0.45343 |
| H(11) | -0.28475 | -0.26921 | 0.45641 |
| H(111) | 0.17125 | -0.16216 | 0.50191 |

τ_9 torsion angle reaches a value between -170 and -167.5° . Consequently, the conformation of the succinate fragment is nearly in the all-trans conformation (t_5). This choice of the PTMTS polyester model is confirmed by a structure factor calculation using the X-ray diffracted intensities. The refinement of the scale factor and an overall isotropic thermal parameter converged, when $R_w = 12.2\%$ and $B = 13.7\ \text{\AA}^2$, for 26 observed reflections. When the 57 unobserved reflections were included, $R_w = 15.3\%$.

A comparable procedure is followed in the case of PTMTA. The agreement between observed and calculated diffraction patterns is optimized by small adjustments of the torsion angles. In doing so, the conforma-

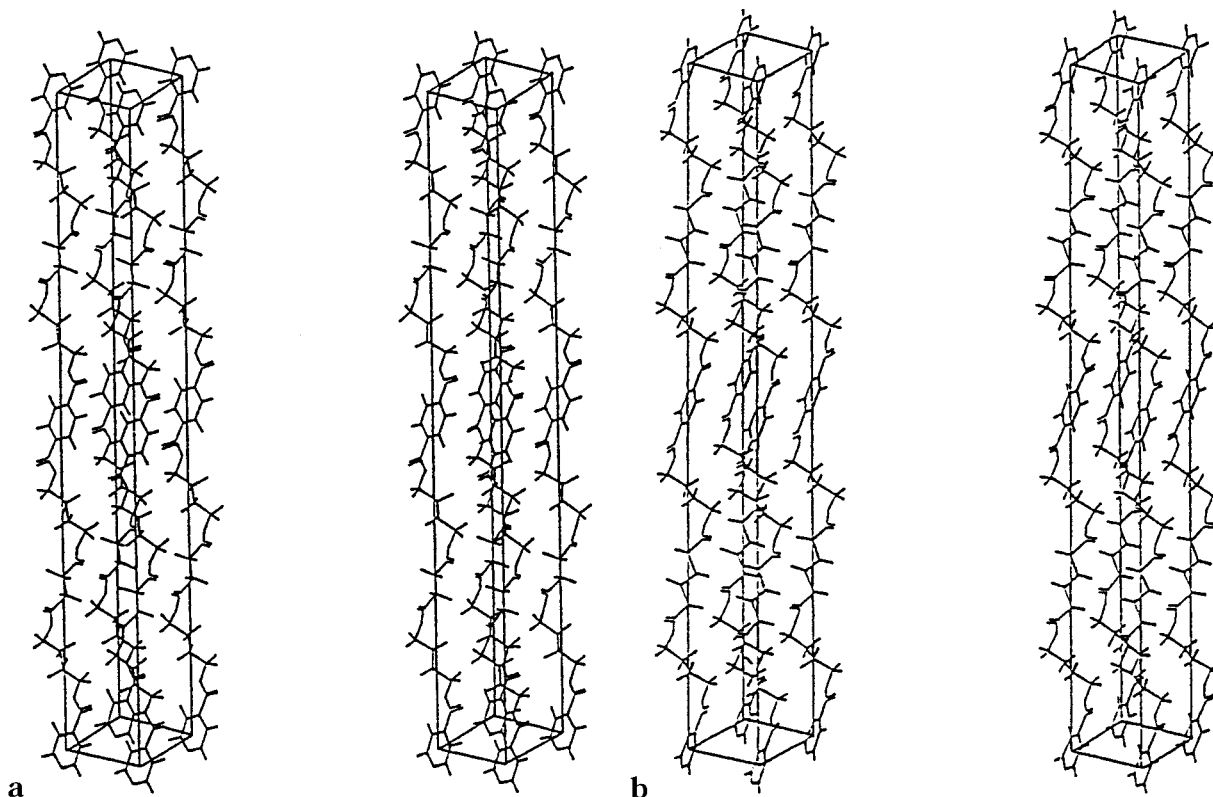


Figure 8. Stereopair showing the packing of the (a) PTMTA and (b) PTMTS chains in their unit cells.

tion of the adipate fragment, defined by the torsion angles τ_8 to τ'_8 , is $ts^{-}tsttst$. The refinement converged, when $R_w = 11.5\%$ and $B = 13.8 \text{ \AA}^2$, for 29 observed reflections. When the 61 unobserved reflections were included, $R_w = 13.5\%$.

The relatively low values taken by the agreement index, R_w , confirm the crystalline structures of PTMTS and PTMTA.

To determine what the range of fluctuation of the torsion angles might be, the chain conformations were minimized within their unit cell, through the Dreiding force field³⁹ and the Polak–Ribiere conjugate gradient.⁴⁰ The maximum displacement of the atomic positions was 0.5 \AA . In the first stage of minimization, the succinate and adipate torsion angles were kept constant at the values given in column 1 of Table 6 while the torsion angles τ_3 – τ_7 of the tetramethylene glycol segment were allowed to vary. The values obtained for these torsion angles at the end of this stage are given in column 2 of Table 6. In the second stage the glycolic torsion angles were kept constant at the values given in column 2 and the diacid torsion angles were allowed to vary. The values obtained for these torsion angles after minimization are given in column 3 of Table 6. Finally all torsion angles were minimized to give the values of column 4, which were compared in Table 7 to those published for 4GT.

In the case of PTMTS, the agreement index was reduced from 16.8 to 15.3% while the torsion angles varied within 2° from their final values. The only exception was for the $O(1)$ – $C(5)$ – $C(6)$ – $C(7)$ torsion angle whose value increased from 112.5 to 118° .

For PTMTA, all the torsion angles remain within 2° of their final values while the agreement index, R_w , was reduced from 19.9 to 13.5%. The most drastic reduction of R_w occurred when the torsion angles in the diacid segments were allowed to vary. Although $\tau_4 = O(1)$ –

$C(5)$ – $C(6)$ – $C(7)$ changed from 93.1 to 90.0° , it was the $O(3)$ – $C(9)$ – $C(10)$ – $C(11)$ torsion angle which changed the most, but by only 6° .

The comparison of the observed and the calculated structure factors for the two polymers is shown in Table 8, while the theoretical and experimental fiber patterns are compared in Figure 2. The fractional atomic coordinates are given in Table 9.

The conformation of PTMTS is described by the $tts^{-}s^{-}tsstttts^{-}s^{-}tsstt$ sequence of torsion angles (τ_1 to τ_{10} and τ'_9 to τ'_1), while that of PTMTA, is $tts^{-}s^{-}tsstts^{-}tts^{-}sts^{-}tsstt$ (τ_1 to τ_{11} and τ'_{10} to τ'_1), where $g^\pm = \pm 60^\circ$, gauche; $s^\pm = \pm 90$ to $\pm 150^\circ$, skew; $t = 180^\circ$, trans.

The Acid Moieties. The tilt angle of the carboxylate group with respect to the aromatic ring, as measured by the τ_1 , τ'_1 , and τ_2 torsion angles is almost the same in both PTMTS and PTMTA as well as in 4GT (α -form). As observed in many benzoates and terephthalates,^{16,20,46,47} the carboxylic group is nearly coplanar with the adjacent aromatic ring and the torsion angle $O=C-O-C = 4.4^\circ$, is in the cis conformation.⁴⁸ However, in the aliphatic carboxylic group, the $O=C-O-C$ torsion angle is 28.5° for PTMTS and 27.3° for PTMTA, which is a fairly large deviation from the cis conformation. Furthermore, all four carboxylic groups are in the *E* conformation.

In a survey of the crystal structures reported in the Cambridge Data file⁴⁹ possessing a succinate group, it is found that in seven out of nine cases, this diacid is in the trans conformation. The range of torsion angles is 170 – 180° . The other two molecules are gauche because of large steric effects. It is clear that the succinate moiety is more rigid than the adipate. Thus, it is expected that in PTMTS, the conformational deviations from all-trans will be restricted to the tetramethylene segment, while it could be spread over the tetramethylene and the adipate moieties in the PTMTA.

Furthermore, in all known polymers containing the succinate group, its conformation is always trans. However, some nontrans torsion angles are located in the diacid portion. Turner-Jones and Bunn²⁸ and Minke and Blackwell³² suggested that the distortions in the poly(ethylene adipate), PEA, and in the α -form of poly(tetramethylene adipate), PTMA, respectively, might be located in the diacid moiety. This was confirmed by Boyd et al.⁵⁰ in their study of the structure and packing in crystalline aliphatic polyesters. The most significant structural feature is the deviation of some torsion angles such as τ_8 and τ_9 (-161 and -167.5°) in PTMTS and τ_8 , τ_9 , and τ_{10} (-156.5 , -141.0 , and 169.5°) in PTMTA, from 180° . These torsion angles contribute to the shortening of the c axis and the stability of the crystal lattice.

The projections of the terephthaloyl residue and the succinic segment of PTMTS, onto the ab plane show (Figure 7a) that the α -carbon atoms of the succinate moiety are located on the projection of the C(2)–C(3) and C(2')–C(3') bonds of the aromatic ring. The projections of the terephthaloyl residue and the adipic segment of PTMTA onto the ab plane, shown in Figure 7b, indicate that the diacid moiety and the aromatic ring are superposed. Furthermore, since the β -carbon atoms match the quaternary aromatic carbon, it follows that the carbon atoms of the two kinds of carbonyl groups are almost superposed. Thus, they are indistinguishable in terms of electron density. The oxygen atoms show a slight deviation in this figure. Thus, these features contribute to the formation of what seems like a double unit cell of α -4GT ($2p_0 = 23.2$ Å), giving rise to diffraction spots located only on the even layer lines. Contrary to the observation in PTMTA, the carboxylate groups of PTMTS are not superimposed. Consequently, many diffraction spots are observed on odd-numbered layer lines, especially the seventh. Very faint reflections are also noted on the fifth, eighth, and ninth layer lines, but their intensities could not be evaluated.

The Tetramethylene Sequence. The conformation of the tetramethylene sequence is described by the torsion angles τ_3 – τ_7 . The actual values taken by these angles are compared in Table 6 to those reported for the relaxed form of 4GT. It is found that the tetramethylene conformation adopted in PTMTA is quite comparable to those reported for α -4GT. All the α -4GT torsion angles, τ_3 and τ_4 , fall in the interval 68 – 94.5° , while the range of torsion angles is 83 – 97° in PTMTA. However, in the case of PTMTS, the two torsion angles τ_3 and τ_4 , which both have values of 118° , depart significantly from the 68 – 97° interval. The larger values of τ_3 and τ_4 in PTMTS may be associated with the presence of the succinate group which, as discussed above, is less flexible than the adipate group. As expected, in both PTMTS and PTMTA, the τ_3 and τ_4 torsion angles differ significantly, by a few degrees, from the τ_6 and τ_7 torsion angles. This was noted in the ^1H and ^{13}C NMR spectra, where the methylene adjacent to the oxygen atoms and the central methylene in the glycolic sequence are not chemically equivalent. The sensitivity of the R values to changes in these torsion angles is illustrated in Table 6 for the PTMTS and PTMTA.

The projections onto the bc plane, of the PTMTS and PTMTA structures, respectively, are shown in parts a and b of Figure 7, while the packing of these poly(tetramethylene terephthalate dicarboxylates) is shown by the stereopairs in parts a and b of Figure 8.

The shortest nonbonded intermolecular C \cdots O ($1 + x$, y , z) distance is 3.37 Å, while the O \cdots C (x , $1 + y$, z) distance is 3.41 Å. The C \cdots C distances are all longer than 3.6 Å, and the H \cdots H distances are larger than 2.3 Å, for the PTMTS. The same values are found in the PTMTA structure. Therefore, the molecules are only held in the crystal by van der Waals interactions.

Conclusion

The incorporation of a long and flexible segment in the poly(terephthalates) leads to polymers which are more soluble in common organic solvent (CHCl_3 , CH_2Cl_2 , THF...) and lowers their melting points, as compared to 4GT. These features confirm that the polyesters are different from 4GT and from their parent aliphatic polyesters. The distribution of the aromatic and aliphatic diacids around the tetramethylene glycol segment was investigated by ^1H and ^{13}C NMR spectroscopy. A number of conformationally sensitive IR bands for the poly(tetramethylene terephthalate dicarboxylates), are assigned following a comparison of the FTIR spectra of 4GT, PTMS, and PTMA. The X-ray fiber diffraction pattern of 4GT and those of PTMTS and PTMTA are practically identical. It is only on the third layer line that differences are clearly noted. The poly(tetramethylene terephthalate dicarboxylates), which crystallize with a triclinic unit cell in the $P1$ space group, have conformations which closely resemble that reported for the α -phase of poly(tetramethylene terephthalate). The chain conformations are $\text{tts}^-\text{s}^-\text{tsstt}$ and $\text{tts}^-\text{s}^-\text{tsstt}$ for PTMTS and PTMTA, respectively.

Acknowledgment. The financial support of the Natural Sciences and Engineering Research Council of Canada and the Fonds pour la formation de chercheurs et l'aide à la recherche are hereby acknowledged.

References and Notes

- (1) Tokiwa, Y.; Suzuki, T. *J. Appl. Polym. Sci.* **1981**, *26*, 441.
- (2) (a) Takota, Y.; Ishioka, R.; Watanabe, N. *Abstract*, 3rd International Scientific Workshop on Biodegradable Plastics and Polymers, Nov. 1993, Osaka, Japan; p 96. (b) Nishoka, M.; Tuziki, T.; Wanajyo, Y.; Oonami, F.; Horiuchi, T. *Abstract*, 3rd International Scientific Workshop on Biodegradable Plastics and Polymers, Nov. 1993, Osaka, Japan; p 97. (c) Sung, K. Y.; Song, D. K. *Polym. Prepr.* **1996**, *37*, 107. (d) Doi, Y.; Kasuya, K.; Abe, H.; Koyama, N.; Ishiwatari, S.; Takagi, K.; Yoshida, Y. *Polym. Degrad. Stab.* **1996**, *51*, 281.
- (3) Bitritto, M. M.; Bell, J. P.; Brenckle, G. M.; Huang, S. J.; Knox, J. R. *J. Appl. Polymer Int.* **1992**, *27*, 213.
- (4) Proter, R. S.; Wang, Li-H. *Polymer* **1992**, *33*, 2019–2030 and references therein.
- (5) (a) MacDonald, W. A.; McLenaghan, A. D. W.; McLean, G.; Richards, R. W.; King, S. M. *Macromolecules* **1991**, *24*, 6164. (b) Kugler, J.; Gilmer, J. W.; Wiswe, D.; Zachmann, H.-G.; Hahn, K.; Fischer, E. W. *Macromolecules* **1987**, *20*, 1116. (c) McAlea, K. P.; Schultz, J. M.; Gardner, K. H.; Wignall, G. D. *Polymer* **1986**, *27*, 1581.
- (6) Jacques, B.; Devaux, J.; Legras, R.; Nield, E. *J. Polym. Sci., Polym. Chem.* **1996**, *34*, 1189–1194 and references therein.
- (7) Manuel, H. J.; Gaymans, R. J. *Polymer* **1993**, *34*, 636.
- (8) El Fary, M.; Slonecki, J. *Angew. Makromol. Chem.* **1996**, *234*, 103–117.
- (9) (a) Wang, L. H.; Lu, M.; Yang, X.; Poreter, R. S. *J. Macromol. Sci., Phys.* **1990**, *B29*, 171. (b) Devaux, J.; Godard, P.; Mercier, J. P. *J. Polym. Sci., Polym. Phys. Ed.* **1986**, *24*, 3301. (c) Godard, P.; Dekoninck, J. M.; Pevlesaver, V.; Devaux, J. *J. Polym. Sci., Polym. Phys. Ed.* **1986**, *24*, 3315. (d) Henrichs, P. M.; Tribone, J.; Massa, D. J.; Hewitt, J. M. *Macromolecules* **1988**, *21*, 1282.
- (10) (a) Park, S. S.; Jeong, J. H.; Im, D. W.; Im, S. S. *Polymer (Korea)* **1996**, *20*, 87. (b) Park, S. S.; Jeong, J. H.; Im, D. W.; Im, S. S. *Polymer (Korea)* **1996**, *20*, 431.
- (11) Yoo, E. S.; Im, S. S. *Macromol. Symp.* **1997**, *118*, 739–745.
- (12) Boye, G. A.; Overton, J. R. *Bull. Am. Phys. Soc.* **1974**, *19*, 352.

- (13) Mencik, Z. *J. Polym. Sci. Polym. Phys. Ed.* **1975**, *13*, 2173.
- (14) Joly, A. H.; Nemoz, G.; Douillard, A.; Vallet, G. *Makromol. Chem.* **1975**, *176*, 479.
- (15) Yokouchi, M.; Sakakibara, Y.; Chatani, Y.; Tadokoro, H.; Tanaka, T.; Yoda, K. *Macromolecules* **1976**, *9*, 266.
- (16) Hall, I. H.; Pass, M. G. *Polymer* **1976**, *17*, 807.
- (17) Desborough, I. J.; Hall, I. H. *Polymer* **1977**, *18*, 825.
- (18) Stambaugh, B.; Koenig, J. L.; Lando, J. B. *J. Polym. Sci., Polym. Phys. Ed.* **1979**, *17*, 1053.
- (19) Ward, I. M.; Wilding, M. A. *Polymer* **1977**, *18*, 327.
- (20) Stambaugh, B.; Lando, J. B.; Koenig, J. L. *J. Polym. Sci., Polym. Phys. Ed.* **1979**, *17*, 1063.
- (21) Gillettes, P. C.; Dirlikov, S. D.; Koenig, J. L.; Lando, J. B. *Polymer* **1982**, *23*, 828.
- (22) Siesler, H. W. *J. Polym. Sci., Polym. Lett. Ed.* **1979**, *17*, 453.
- (23) Tashiro, K.; Nakai, Y.; Kobayashi, M.; Tadokoro, H. *Macromolecules* **1980**, *13*, 137.
- (24) Fuller, C. S. *Chem. Rev.* **1940**, *26*, 143.
- (25) Kanamoto, T.; Tanaka, K. *J. Polym. Sci., Part A-2*. **1971**, *9*, 2043.
- (26) Fuller, C. S.; Erickson, C. L. *J. Am. Chem. Soc.* **1937**, *59*, 344.
- (27) Ueda, A. S.; Chatani, Y.; Tadokoro, H. *Polym. J.* **1971**, *2*, 387.
- (28) Turner-Jones, A.; Bunn, C. W. *Acta Crystallogr.* **1962**, *15*, 105.
- (29) Ihn, K. J.; Yoo, E. S.; Im, S. S. *Macromolecules* **1995**, *28*, 2460.
- (30) Ichikawa, Y.; Suzuki, J.; Washiyama, J.; Moteki, Y.; Noguchi, K.; Okuyama, K. *Polymer* **1994**, *35*, 3338.
- (31) Ichikawa, Y.; Washiyama, J.; Moteki, Y.; Noguchi, K.; Okuyama, K. *Polym. J.* **1995**, *27*, 1230.
- (32) Minke, R.; Blackwell, J. *J. Macromol. Sci. Phys.* **1979**, *B16*, 407.
- (33) Turrarandi, L.; Barandiarán, M. J.; Asúa, J. M. *Polymer* **1988**, *29*, 971.
- (34) Jing-Sheng Bao, Hong-Ni Fan. *Polym. Int.* **1992**, *27*, 213.
- (35) For general reviews of the synthesis of polyesters: Sorenson, W.; Campbell, T. W. *Preparative Methods of Polymer Chemistry*, Intersciences Publishers: New York, 1961.
- (36) Billmeyer, F. W.; Alan, D. E. *Macromolecules* **1969**, *2*, 103.
- (37) McNeil, I. C.; Bounekhel, M. *Polymer Degrad. Stab.* **1991**, *34*, 187.
- (38) Palmer, A.; Poulin-Dandurand, S.; Brisse, F. *Can. J. Chem.* **1985**, *63*, 3079.
- (39) Mayo, S. L.; Olafson, B. D.; Goddard, W. A. *J. Phys. Chem.* **1990**, *94*, 8897.
- (40) Fletcher, R.; Reeves, C. M. *Comput. J.* **1964**, *7*, 149.
- (41) Cromer, D. J.; Mann, J. B. *Acta Crystallogr.* **1968**, *A24*, 321.
- (42) Stewart, R. F.; Davidson, E. R.; Simpson, W. T. *J. Chem. Phys.* **1970**, *53*, 1891.
- (43) ^1H NMR (CDCl_3 , ppm) of: $\text{H}_3\text{CO}-\text{CO}-(\text{CH}_2)_2-\text{CO}-\text{O}-(\text{CH}_2)_4-\text{O}-\text{CO}-\text{C}_6\text{H}_4-\text{CO}-\text{O}-(\text{CH}_2)_4-\text{O}-\text{CO}-(\text{CH}_2)_2-\text{CO}-\text{OCH}_3$: 1.82–1.86 (8H, m), 2.64 (8H, s), 3.69 (6H, s), 4.18 (4H, t), 4.38 (4H, t), 8.10 (4H, 1s).
- (44) (a) Grenier-Loustalot, M. F.; Bocelli, G. *Eur. Polym. J.* **1984**, *19*, 957. (b) Gomez, M. A.; Cozine, M. H.; Tonelli, A. E. *Macromolecules* **1988**, *12*, 388.
- (45) For example in the PTMS ^1H NMR (CDCl_3), three signals are shown at 1.7 and 4.1 ppm ($-\text{CH}_2-$ of the 1,4-butanediol unit) and 2.6 ppm ($-\text{CH}_2-$ of the succinyl unit).
- (46) Sasaki, S.; Takigawa, S. *J. Polym. Sci.* **1989**, *B27*, 1077.
- (47) Li, X. Ph.D. Thesis, Université de Montréal, Montréal, Québec, Canada 1993.
- (48) (a) Hall, I. H. In *Structure of Crystalline Polymers*; Hall, I. H., Ed.; Elsevier Applied Science: New York, **1984**. (b) Wilberg, K. B.; Laidig, K. E. *J. Am. Chem. Soc.* **1987**, *109*, 5935. (c) Blom, C. E.; Günthard, Hs. H. *Chem. Phys. Lett.* **1981**, *84*, 267.
- (49) Cambridge Data File, Molecular codes: BEKJIK, DPSUC, HEGKAF, MCMSA10, SUCCHO, SUCHLO, SUCPIC10, VEBYEG, and WAJPUS10.
- (50) Liau, W. B.; Boyd, R. H. *Macromolecules* **1990**, *23*, 1531.

MA991375B